International Journal of Innovative Research and Scientific Studies, 8(3) 2025, pages: 12-29

IJIRSS
International Journal of Innovative Research & Scientific Studies

ISSN: 2617-6548

URL: www.ijirss.com



Catalytic conversion of palm acid oil and bulk cooking oil to biodiesel using Fe/aluminosilicate

Widayat Widayat[1,2*], Rani Amelia Sumarno[1], Yufridha Yuni Ananda[1], Sulardjaka Sulardjaka[3], John Philia[2]

[1]*Department of Chemical Engineering, Faculty of Engineering, Diponegoro University, Semarang 50275, Indonesia.*
[2]*Advanced Material Laboratory, Diponegoro University, Semarang 50275, Indonesia.*
[3]*Department of Mechanical Engineering, Faculty of Engineering, Diponegoro University, Semarang 50275, Indonesia.*

Corresponding author: Widayat Widayat (*Email: widayat@live.undip.ac.id*)

Abstract

The conversion of palm acid oil and bulk cooking oil into biodiesel presents considerable opportunities while employing catalysts. The development of effective catalysts, which may improve both esterification and transesterification processes, is essential for optimizing biodiesel production from these feedstocks. This study investigates biodiesel production from a mixture of palm acid oil (PAO) and bulk cooking oil using an Fe/aluminosilicate catalyst synthesized via the wet impregnation method. Fe was derived from iron sand, while geothermal waste was employed as a source of aluminosilicate silica. The optimization of biodiesel conversion was conducted using the Central Composite Design (CCD) approach, with catalyst concentration, reaction temperature, and Fe/aluminosilicate molar ratio as the key variables. Catalyst characterization was performed using SEM-EDX and XRD to analyze its structural and elemental composition. The results indicate that the highest biodiesel conversion of 90.2976% was achieved under the optimal conditions of 2% catalyst concentration, a reaction temperature of 65°C, and an Fe/aluminosilicate molar ratio of 1:12. The findings demonstrate the potential of Fe/aluminosilicate catalysts derived from geothermal waste to improve biodiesel production efficiency while promoting sustainable industrial waste utilization.

Keywords: Biodiesel, Central composite design, Fe/Aluminosilicate, Heterogeneous catalyst, Wet impregnation.

DOI: 10.53894/ijirss.v8i3.6425
Funding: This project was supported and funded by World Class Research Diponegoro University (Grant Number: SPK 357-39/UN7.D2/PP/IV/2024).
History: Received: 3 March 2025 / **Revised:** 4 April 2025 / **Accepted:** 7 April 2025 / **Published:** 24 April 2025
Copyright: © 2025 by the authors. This article is an open access article distributed under the terms and conditions of the Creative Commons Attribution (CC BY) license (https://creativecommons.org/licenses/by/4.0/).
Competing Interests: The authors declare that they have no competing interests.
Authors' Contributions: All authors contributed equally to the conception and design of the study. All authors have read and agreed to the published version of the manuscript.
Transparency: The authors confirm that the manuscript is an honest, accurate, and transparent account of the study; that no vital features of the study have been omitted; and that any discrepancies from the study as planned have been explained. This study followed all ethical practices during writing.
Publisher: Innovative Research Publishing

1. Introduction

Over the past century, the rapid increase in greenhouse gas concentrations has intensified global warming and climate disruptions, primarily driven by fossil fuel combustion in the energy and transportation sectors [1, 2]. The depletion of fossil fuel reserves, coupled with volatile global oil prices, has necessitated the exploration of sustainable energy alternatives [3, 4]. Biodiesel, a renewable and environmentally friendly fuel, has emerged as a viable substitute due to its compatibility with conventional combustion engines without significant modifications [5]. Among various feedstocks, palm acid oil (PAO), a byproduct of palm oil refining, presents economic and environmental advantages due to its high free fatty acid (FFA) content (>50%), predominantly in the form of palmitic acid [6, 7]. Its widespread availability and low cost make PAO a promising raw material for biodiesel production [8]. Additionally, bulk cooking oil, a low-grade triglyceride, is gaining interest as a biofuel feedstock, demonstrating an optimal biodiesel yield of 87.6% [9].

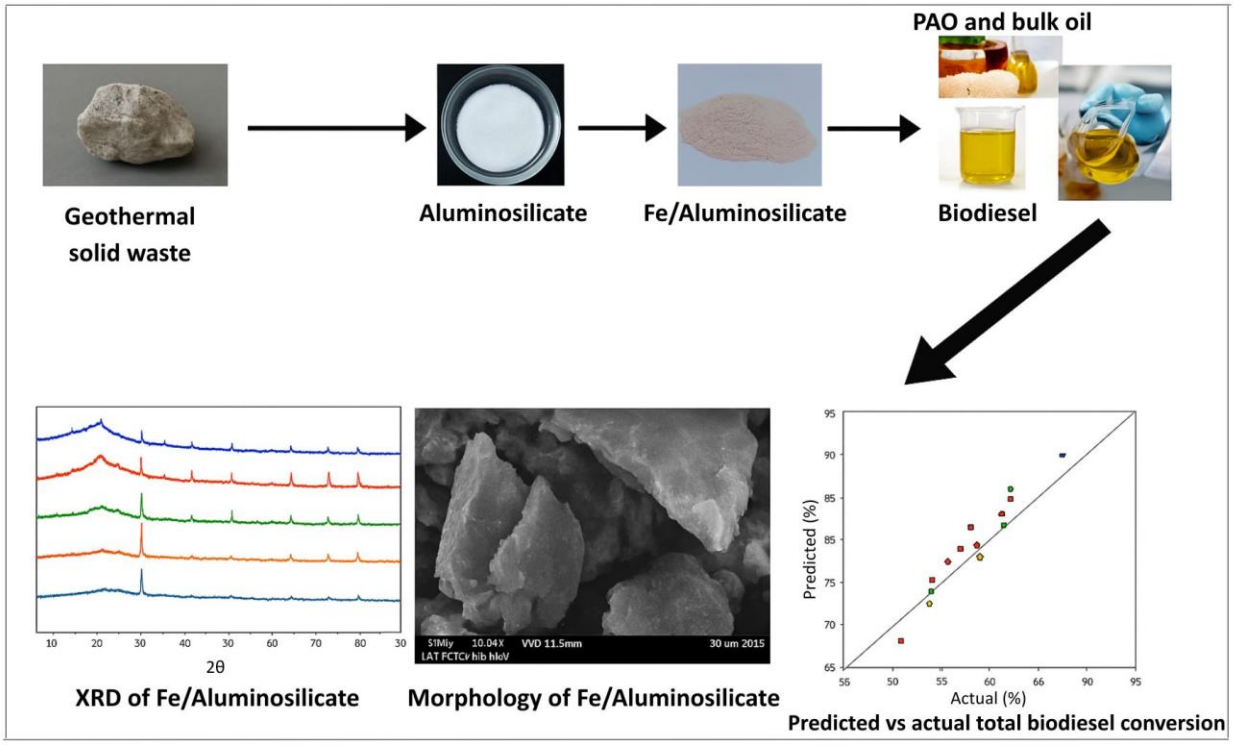


Figure 1.
Graphical abstract.

Catalysts are essential in biodiesel synthesis, significantly enhancing reaction kinetics and conversion efficiency. Heterogeneous catalysts are favored over homogeneous ones due to their superior recyclability, ease of recovery, and lower soap formation, which minimizes contamination and production costs [10-12]. To address the limitations of acidic and basic heterogeneous catalysts, bi-functional catalysts have been developed, capable of simultaneously facilitating both esterification and transesterification reactions. These catalysts effectively mitigate the adverse effects of high free fatty acid (FFA) and water content by incorporating amphoteric support materials modified with active acidic or basic promoters [13]. Moreover, heterogeneous catalysts are highly sustainable due to their recyclability, reusability, low toxicity, and minimal energy demands, making them ideal for environmentally friendly biodiesel production [14].

Among transition metals, iron (Fe) exhibits a strong affinity for aluminosilicate frameworks, allowing its incorporation during aluminosilicate crystallization with greater efficiency than other transition metals. The integration of Fe into the aluminosilicate matrix enhances catalytic performance by introducing key functional properties, including hydrophobicity, tunable acidity, and redox activity, which are critical for oxidation-reduction reactions and other catalytic applications [15]. Prior studies have demonstrated the effectiveness of Fe-modified zeolite in biodiesel production, achieving high FFA conversion efficiencies. Lani et al. [16] in Gupta and Singh [17] employed CaO–ZSM5 aluminosilicate/Fe_3O_4 catalysts derived from eggshell waste and rice straw on waste cooking oil, yielding a maximum biodiesel yield of 91%. Catalyst supports play a crucial role in optimizing the performance of heterogeneous catalysts by significantly increasing their specific surface area and providing a well-defined porous structure to accommodate active sites [18]. The impregnation of metal species onto these supports enhances catalytic reactivity and selectivity, facilitating more efficient catalytic transformations. Various impregnation techniques enable the deposition of metal oxides onto catalyst supports, with the selection of metal precursors and charge states influencing the physicochemical properties of the final catalyst [19].

Geothermal waste, particularly its high silica content, presents a valuable resource for aluminosilicate synthesis, offering both economic and environmental benefits. Aluminosilicates with porous structures exhibit exceptional catalytic properties due to their high internal surface area and thermal stability [16]. Amorphous silica, a predominant component of geothermal waste alongside sodium and potassium chloride, serves as a key precursor for aluminosilicate production [20]. Converting geothermal waste into aluminosilicates improves resource efficiency and mitigates waste disposal issues, following

sustainable waste management practices. Additionally, geothermal operations often encounter scaling issues caused by mineral deposits, primarily silica, calcium compounds, and sulfides, which impede equipment efficiency [21]. Since silica concentration in geothermal waste correlates with condensate temperature, its extraction and transformation into aluminosilicates provide a dual advantage—reducing scaling in geothermal systems while producing high-value materials for catalytic and adsorption applications [22]. This approach not only mitigates industrial scaling challenges but also promotes a circular economy by converting waste into functional materials.

To the best of our knowledge, this study aims to optimize biodiesel production from a PAO-bulk oil mixture using Fe/aluminosilicate catalyst. This study involves extracting Fe from iron sand and synthesizing aluminosilicate from geothermal waste. The development of this catalyst offers a solution rooted in circular economy principles, promoting the efficient use of natural resources and industrial waste. The optimization investigation focuses on evaluating critical process parameters, including catalyst concentration, operating temperature, and catalyst-to-oil ratio, to maximize biodiesel yield and efficiency. A Central Composite Design (CCD) approach is employed to systematically analyze parameter interactions and determine optimal reaction conditions. This study contributes to the development of sustainable catalytic systems, bridging the gap between industrial waste valorization and biodiesel production for enhanced energy security and environmental sustainability.

2. Materials and Methods

2.1. Materials

The primary raw materials utilized in this study include palm acid oil (PAO) sourced from the Palm Oil Industry and bulk cooking oil obtained from the Manyaran Market, Semarang, Central Java. The free fatty acid (FFA) content analysis revealed that PAO contained 68.53% FFA, while bulk oil had a significantly lower FFA content of 0.16%. Aluminosilicate was derived from geothermal waste obtained from PT. Geodipa Energi, Dieng, whereas iron (Fe) was extracted from iron sand. The chemical reagents used in the catalyst synthesis process included methanol and polyethylene glycol (PEG 4000) (technical grade), along with 37% hydrochloric acid (HCl), 25% ammonium hydroxide (NH_4OH), 98% sulfuric acid (H_2SO_4), aluminum sulfate ($Al(SO_4)_3 \cdot 18H_2O$), and sodium hydroxide (NaOH) (analytical grade, Merck). The synthesis of aluminosilicate was carried out using a hydrothermal reactor. The experimental setup consisted of a 250 mL three-neck flask, magnetic stirrer, heater, thermometer, water bath, condenser (reflux system), and supporting laboratory apparatus such as stands and clamps, as illustrated in Figure 2, which were used for biodiesel production.

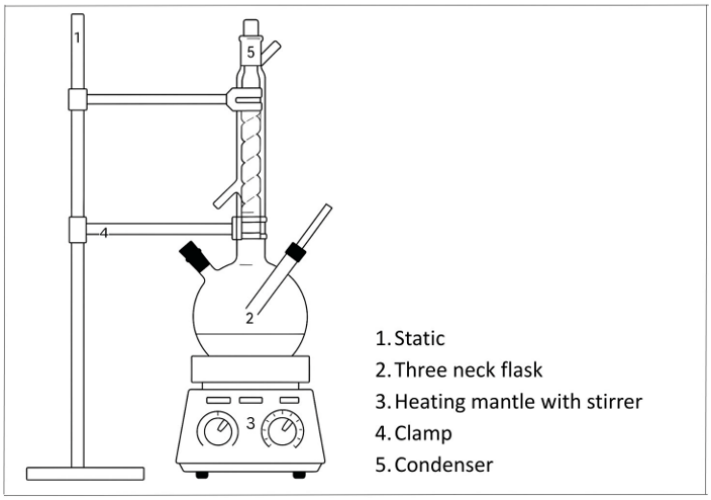


Figure 2.
Main equipment.

2.2. Methods

2.2.1. Fe/Aluminosilicate Catalyst Synthesis

Aluminosilicate, synthesized from sodium silicate, which is produced from geothermal waste. A total of 500 grams of geothermal waste was combined with 2 liters of a 0.6% hydrochloric acid (HCl) solution and agitated at a rate of 100 rpm for 30 minutes to facilitate the dissolution of metal impurities. The filtration process was subsequently employed to separate the solid geothermal waste from the liquid phase. The solid residue obtained underwent a washing process with deionized water until the pH level was adjusted to 7, thereby confirming the elimination of any residual acid and impurities. The geothermal waste underwent a washing process followed by drying in an oven at a temperature of 200 °C for 1 hour to remove any remaining moisture. The dried sample underwent calcination at a temperature of 850 °C for 3 hours to remove organic compounds and sulfur content.

Aluminosilicate was produced through the reaction of sodium silicate as a silica source, aluminium sulfate as an alumina source, and H_2O. The synthesis process commenced with the formulation of sodium silicate derived from geothermal waste and a sodium hydroxide solution. In the synthesis of sodium silicate, 250 grammes of purified geothermal waste were solubilised in 1000 mL of 2 N sodium hydroxide (NaOH) solution. The solution was agitated with a magnetic stirrer at a velocity of 300 rpm and maintained at a temperature of 30 °C for 2 hours. While the aluminium sulfate solution was produced

through the dissolution of $Al(SO_4)_2 \cdot 18H_2O$ in H_2SO_4. The precursor mixture has a pH of 11, with a SiO_2/Al_2O_3 molar ratio of 40, OH/SiO_2 of 0.03, and H_2O/SiO_2 of 43. The materials are combined in a specified ratio until a uniform mixture is achieved. Subsequently, a hydrothermal treatment is conducted utilising an autoclave reactor, maintained at a temperature of 125°C for 6 hours.

Fe is extracted from iron sand with a slight modification of the method from Prameswari et al. [23]. The Fe/aluminosilicate catalyst is prepared via the wet impregnation method. A specific quantity of Fe precursor was dissolved in deionized water and subsequently mixed with aluminosilicate to obtain Fe to aluminosilicate mass ratio 1:6.6, 1:8, 1:10, 1:12, and 1:13.3. The mixture was stirred at 60 °C for 6 hours at a stirring speed of 500 rpm to ensure homogenous dispersion of the Fe precursor on the aluminosilicate. The solvent was then evaporated by using an oven at 110 °C for 12 hours, followed by calcination at 550 °C for 6 hours. Characteristics of the catalyst were observed by XRD, SEM-EDX and physisorption analysis.

2.2.2. Biodiesel Production

Production of biodiesel from palm acid oil and bulk oil was carried out through the transesterification process. The transesterification process is carried out at a methanol-to-oil molar ratio of 12:1 for 5 hours. The catalyst was first combined with methanol and allowed to mix for 30 minutes, subsequently followed by the addition of a blend of palm acid oil and bulk oil in a 1:1 ratio. This study employs catalyst concentrations of 2%, 3%, and 4% to optimize biodiesel yield while preventing excessive viscosity and undesired saponification [24, 25]. The reaction temperatures of 55°C, 60°C, and 65°C are selected based on methanol's boiling point (64.7°C) to balance reaction kinetics, ensure efficient methanol utilization, and minimize energy consumption [26]. The catalyst loading, catalyst type, and reaction temperature were set according to the variables. Post-reaction, phase separation is performed using a separatory funnel, followed by centrifugation to enhance product purity.

2.3. CCD Method

The Central Composite Design (CCD) is a widely utilized fractional factorial design in response surface methodology (RSM), facilitating the optimization of process parameters by incorporating center points and a set of axial (star) points to assess curvature effects. CCD enables the construction of a second-order polynomial regression model, allowing for the estimation of regression coefficients and the interaction effects of independent variables on the response [27]. This approach enhances the accuracy of predicting optimal operating conditions while minimizing the number of experimental runs required.

The determination of the axial (star) points in CCD involves computing the alpha (α) value, which defines the position of these points relative to the factorial region. The alpha value (α) is calculated using the following equation:

$$\alpha = (2^k)^{0,25} \tag{1}$$

where k represents the number of independent variables in the experimental design. The calculated α value ensures appropriate spacing of experimental points, improving the robustness of the response surface model in capturing nonlinear effects.

The response variable in this study is the total biodiesel conversion, which is quantitatively analyzed using gas chromatography-mass spectrometry (GC-MS) to determine the fatty acid methyl ester (FAME) content. The total conversion is calculated using the following equations:

$$\text{Esterification conversion } (\%) = \left[\frac{\%\text{FFA} - \%\text{FFA total}}{\%\text{FFA total}}\right] \times 100\% \tag{2}$$

$$\text{TG conversion } (\%) = \left(\text{initial mole TG} - \frac{\text{transesterification mole ME}}{3}\right) \times 100\% \tag{3}$$

$$\text{Total conversion } (\%) = \%\text{Esterification conversion} + \%\text{TG conversion} \tag{4}$$

To establish the relationship between the dependent (response) variable and independent (predictor) variables, response surface methodology (RSM) utilizes polynomial regression models. These models provide a mathematical framework for analyzing experimental data and optimizing process parameters. The general form of the polynomial regression equation in RSM is expressed as:

$$Y = \beta_0 + \beta_1 X_1 + \cdots + \beta_k X_k + \beta_{12} X_1 X_2 + \beta_{13} X_1 X_3 + \cdots + \beta_{k-1}, kX_{k-1} X_k + \beta_{11} {X_1}^2 + \cdots + \beta_{kk} {X_k}^2 + \epsilon \tag{5}$$

Where:
Y = dependent variable/outcome variable/estimated response
$X_1,\ldots X_k$ = independent variables
X_1X_2, $X_1X_3,\ldots$, X_{k-1}, X_k = interaction of independent variables
${X_1}^2,\ldots {X_k}^2$ = the square of the independent variables
β_0 = overall mean response/intercept constant
β_1 = regression model coefficient
k = number of independent variables
ϵ = error

In this study, the regression analysis results are implemented in the polynomial equation, with the total biodiesel conversion as the response variable. The predictor variables include catalyst concentration (X_1), operating temperature (X_2), and catalyst ratio (X_3). This model enables the prediction and optimization of biodiesel production conditions by evaluating

the influence of individual parameters and their interactions. Table 1 presents the experimental design, while the regression analysis and ANOVA results were provided by Tables 2 dan Table 3.

Table 1.
Experimental Variable Design.

Run	Code variable			Practical variable		
	X_1	X_2	X_3	% Catalyst	Temperature (°C)	Catalyst ratio
1	-1	+1	-1	2	65	8
2	-1	+1	+1	2	65	12
3	-1	-1	+1	2	55	12
4	-1	-1	-1	2	55	8
5	0	0	0	3	60	10
6	0	0	0	3	60	10
7	+1	+1	-1	4	65	8
8	+1	-1	-1	4	55	8
9	+1	+1	+1	4	65	12
10	+1	-1	+1	4	55	12
11	+1,682	0	0	4,681.79	60	10
12	-1,682	0	0	1,31821.	60	10
13	0	-1,682	0	3	51,5911.	10
14	0	0	-1,682	3	60	6,636.42
15	0	+1,682	0	3	68,4089.	10
16	0	0	+1,682	3	60	13,3636.

Table 2.
Regression Analysis Results.

Parameter	Regression coefficient	Standard Error	95% Confidence Interval Low	95% Confidence Interval High
Intercept	85.54	0.3444	84.69	86.38
X_1	0.3119	0.1322	-0.0116	0.6354
X_2	1.45	0.1322	1.12	1.77
X_3	0.8532	0.1322	0.5297	1.18
$X_1 X_2$	-0.3321	0.1727	-0.7547	0.0906
$X_1 X_3$	-1.09	0.1727	-1.51	-0.6641
$X_2 X_3$	0.0736	0.1727	-0.349	0.4963
X_1^2	0.5485	0.1605	0.1557	0.9412
X_2^2	0.5026	0.1605	0.1098	0.8953
X_3^2	-0.1965	0.1605	-0.5893	0.1962

Table 3.
ANOVA.

Parameter	Sum of Squares	Degrees of Freedom	Mean Square	F-statistic	p-value
Model	57.01	9	6.33	26.54	0.0004
X_1	1.33	1	1.33	5.57	0.0564
X_2	28.56	1	28.56	119.67	< 0.0001
X_3	9.94	1	9.94	41.65	0.0007
$X_1 X_2$	0.8822	1	0.8822	3.70	0.1029
$X_1 X_3$	9.45	1	9.45	39.58	0.0008
$X_2 X_3$	0.0434	1	0.0434	0.1817	0.6848
X_1^2	2.79	1	2.79	11.68	0.0142
X_2^2	2.34	1	2.34	9.80	0.0203
X_3^2	0.3578	1	0.3578	1.50	0.2667
Residual	1.43	6	0.2387		
Lack of Fit	1.36	5	0.2715	3.65	0.3771
Pure Error	0.0745	1	0.0745		
Total	58.44	15			

3. Results and Discussion

3.1. Free Fatty Acid Content of The Feedstock

Free Fatty Acid (FFA) refers to fatty acids that exist in a free state, unbound to glycerol molecules as triglycerides. The FFA content is a critical parameter in biodiesel production, as it directly influences the efficiency of the transesterification process. In this study, palm acid oil (PAO) exhibits an exceptionally high FFA content of 68.53%, whereas bulk cooking oil contains only 0.16% FFA. According to Chiedu et al. [28], an increase in FFA content correlates with a reduction in total biodiesel conversion due to the competitive formation of soap via saponification reactions, which hinder ester formation. The presence of excessive FFA leads to unwanted side reactions, reducing the efficiency of the transesterification process and negatively impacting biodiesel yield [29]. Therefore, it is necessary to reduce the FFA content before transesterification to enhance biodiesel yield and prevent catalyst deactivation. In this study, a 1:1 volume ratio mixture of PAO and bulk cooking oil results in a blended feedstock with an FFA content of 20.68%, which is more manageable for subsequent esterification and transesterification reactions.

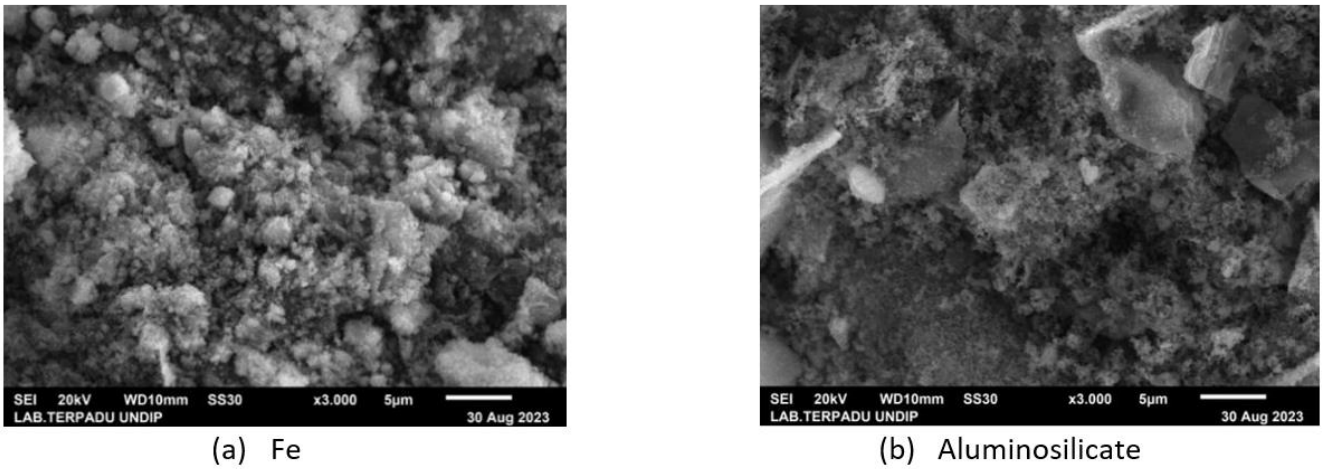
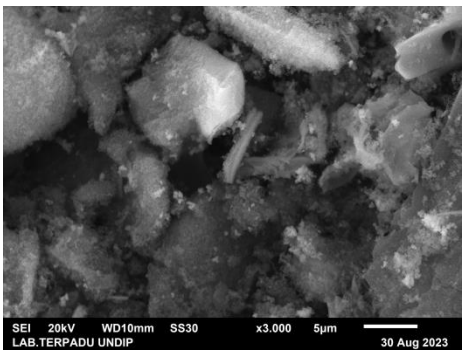


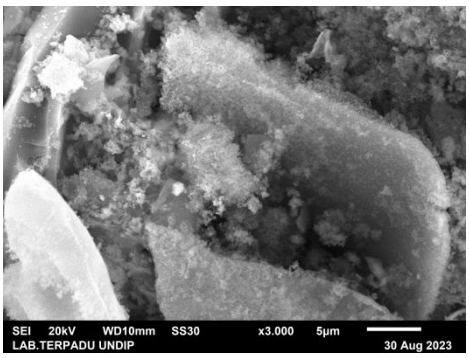
Figure 3.
Morphology and structure of Fe catalyst and aluminosilicate before wet impregnation at x3000 magnification.

3.2. Fe/Aluminosilicate Catalyst Characterization

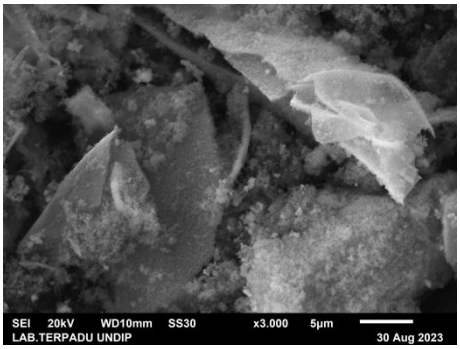
The morphological and structural characteristics of the catalysts were analyzed using Scanning Electron Microscopy-Energy Dispersive X-ray Spectroscopy (SEM-EDX) to examine surface topography, elemental composition, and dispersion of Fe on the aluminosilicate support. Figure 3 illustrates SEM-EDX images of Fe and aluminosilicate before wet impregnation, revealing distinct morphological differences. The Fe structure appears as small, irregular aggregates, while aluminosilicate exhibits a crystalline framework with relatively low crystallinity. These findings indicate that wet impregnation is necessary to ensure uniform Fe dispersion on the aluminosilicate surface, enhancing catalyst effectiveness in biodiesel synthesis.



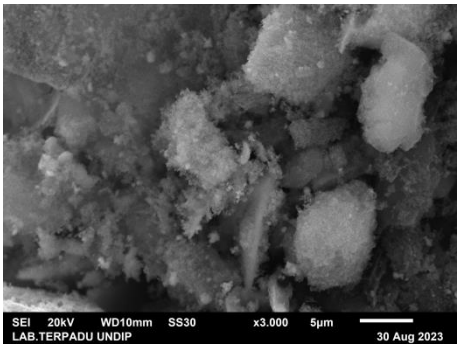
SEM Ratio of 1:8



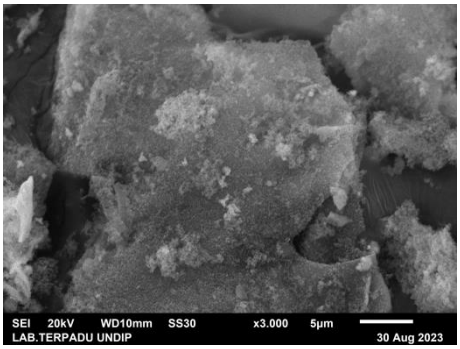
SEM Ratio of 1:10



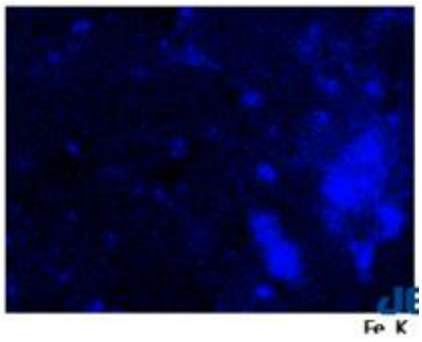
SEM Ratio of 1:12



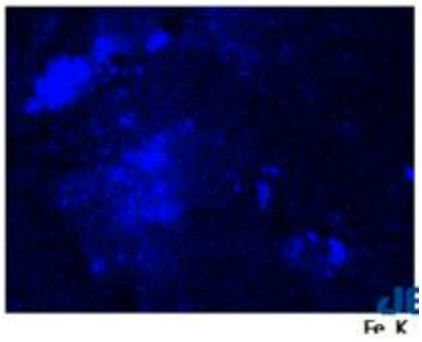
SEM Ratio of 1:6,6



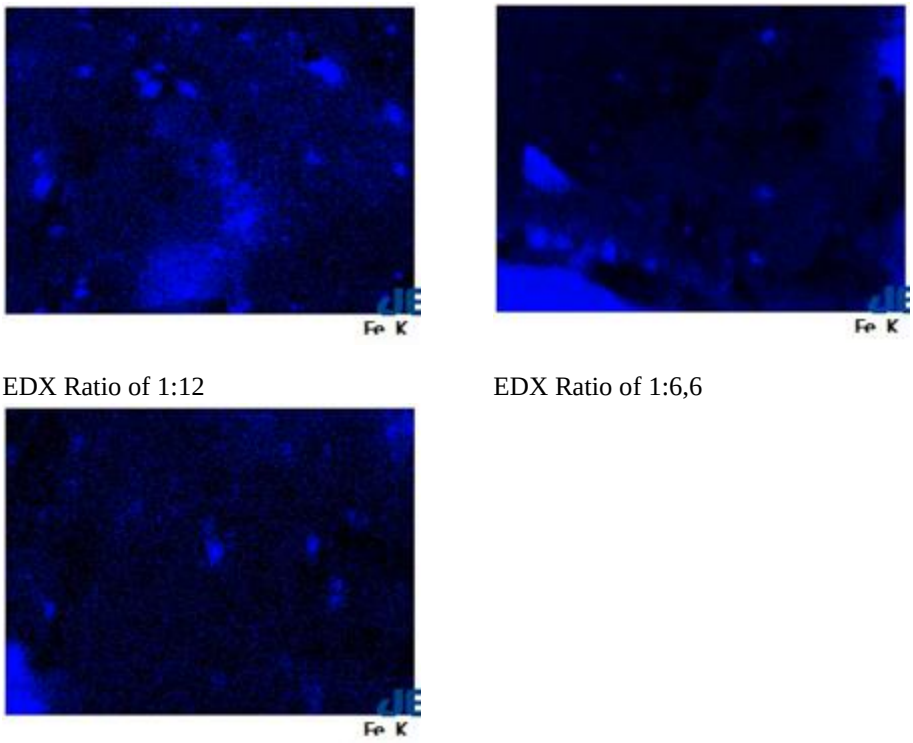
SEM Ratio of 1:13,3



EDX Ratio of 1:8



EDX Ratio of 1:10



EDX Ratio of 1:12

EDX Ratio of 1:6,6

EDX Ratio of 1:13,3

Figure 4.
Morphology and structure of Fe/aluminosilicate catalyst after wet impregnation at x3000 magnification.

Based on Figure 4, the morphological differences of the Fe/aluminosilicate catalyst after wet impregnation at various Fe-to-aluminosilicate ratios can be analyzed. The post-impregnation Fe/aluminosilicate catalyst exhibits an irregular spherical morphology, with particles that tend to agglomerate and exhibit non-uniform sizes, consistent with observations by Putra et al. [30].

At an Fe-to-aluminosilicate ratio of 1:8, the catalyst presents smaller, irregular, and hollow crystals, with small Fe aggregates dispersed across the structure, similar to the Fe morphology observed in Figure 3. At a ratio of 1:10, the catalyst exhibits larger crystal structures, albeit with uneven size distribution, leading to the formation of cavities in certain areas. Compared to 1:8, a higher number of small Fe aggregates are visible. The morphology at a ratio of 1:12 closely resembles that of 1:10, but with a more compact inter-crystal arrangement and a more uniform Fe distribution on the aluminosilicate surface.

A ratio of 1:6.6 results in larger crystals with some smaller forms and a relatively close inter-crystal spacing, but with fewer Fe aggregates compared to 1:8. The Fe/aluminosilicate catalyst at 1:13.3 exhibits the largest and most homogeneous crystals, with minimal inter-crystal cavities, signifying a high degree of structural integrity. However, this ratio also contains the lowest number of Fe aggregates on the aluminosilicate surface, suggesting a lower Fe loading efficiency compared to other ratios.

The distribution of Fe within the aluminosilicate matrix significantly impacts the overall catalytic morphology and performance. A uniform Fe dispersion is crucial for achieving optimal catalytic activity, as it enhances active site availability and reaction efficiency [19]. Based on morphological analysis and Fe distribution, the Fe content ranking across different catalyst ratios, from highest to lowest, follows the order: 1:12 > 1:10 > 1:8 > 1:6.6 > 1:13.3.

The X-ray diffraction (XRD) technique was employed to analyze the phase composition and crystal structure of Fe/aluminosilicate catalysts. This method exploits the interaction between the material and X-rays, which results in diffraction patterns that provide valuable insights into the crystalline nature of the samples. The resulting diffractogram from the XRD analysis of the Fe/aluminosilicate catalysts is shown in Figure 5.

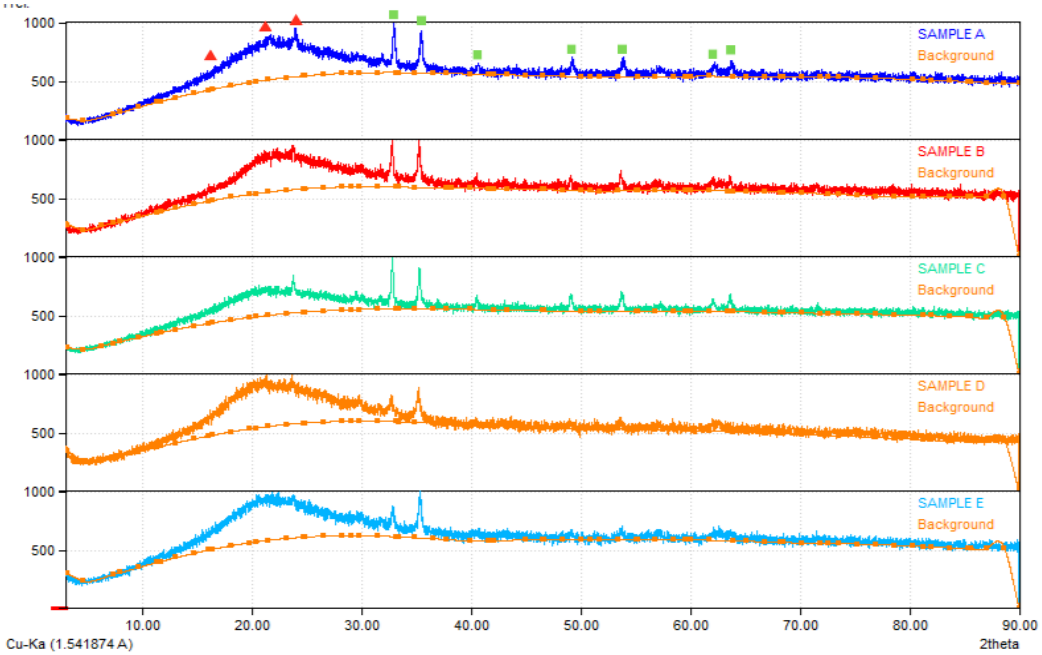


Figure 5.
Fe/aluminosilicate diffractograms (a) 1:8 ratio, (b) 1:10 ratio, (c) ratio 1:12, (d) ratio 1:6.6, (e) ratio 1:13.3

An analysis using X-ray diffraction (XRD) was performed to investigate the phase composition of Fe/aluminosilicate catalysts, with the interpretation of data carried out through Match! software. The investigation of the diffraction patterns revealed the existence of two primary crystalline phases, tridymite (SiO_2) and haematite (Fe_2O_3). These minerals are represented by red triangles and green squares, respectively, in the diffraction patterns. The relative proportions of tridymite and hematite phases are critical in determining the catalytic performance, with an optimal balance potentially contributing both to the structural stability (tridymite) and enhanced reactivity (hematite) of the catalyst [31, 32]. A well-balanced composition of these phases can potentially optimize catalytic performance by ensuring both mechanical robustness and active surface sites for reactions.

Table 4.
Physisorption Analysis of Aluminosilicate and Fe/Aluminosilicate.

Sample	Surface Area (m^2/g)	Total Pore Volume (cm^3/g)	Average Pore Radius (nm)
Aluminosilicate	556.646	1.296	4.656
Fe/Aluminosilicate	423.051	1.1664	3.9576

Data from Table 4 shows the significant differences between aluminosilicate and Fe/aluminosilicate surface area, total pore volume, and average pore distribution. The Brunauer-Emmett-Teller (BET) method was applied to determine the total surface area, while the total pore volume was determined by measuring the amount of nitrogen adsorbed at P/Po 0,994. This alteration represents the pore structure modification caused by the impregnation process. The decrease of surface area after the impregnation process may occur due to pore blockage by Fe particles. The distribution of Fe particles within the aluminosilicate pores covers the surface area of the pores. The aggregation of Fe particles blocks some of the pores and lowers the surface area [33]. Reduction in pore volume and diameter are associated with pore blockage by the Fe particles [34]. Overall, the Fe impregnation altered the pore structure, which likely modified the material properties, yet it enhanced the catalytic activity for biodiesel production [23].

3.3. Biodiesel Production

Biodiesel production from vegetable oils containing free fatty acids (FFAs) can be achieved through a simultaneous esterification and transesterification process involving methanol. This process results in the formation of fatty acid methyl esters (FAME), which constitute the biodiesel product. The chemical reactions that take place are as follows:

Esterification:

$$\underset{\text{(Free Fatty Acid)}}{\text{FFA}} + \underset{\text{(Methanol)}}{CH_3OH} \rightarrow \underset{\text{(Fatty Acid Methyl Esters)}}{\text{FAME}} + \underset{\text{(Water)}}{H_2O}$$

Transesterification:

$$\underset{\text{(Triglycerides)}}{\text{TG}} + \underset{\text{(Methanol)}}{3CH_3OH} \rightarrow \underset{\text{(Fatty Acid Methyl Esters)}}{3\text{FAME}} + \underset{\text{(Glycerols)}}{\text{GL}}$$

[35]

These two reactions, esterification and transesterification, both lead to the formation of biodiesel in the form of fatty acid methyl esters (FAME). However, the extent of FAME production in each reaction is influenced by factors such as the concentration of FFAs and triglycerides, the molar ratio of methanol to oil, the type of catalyst, and the reaction conditions.

To determine the total biodiesel yield, it is necessary to calculate the conversion rates of both reactions. The overall biodiesel conversion can be expressed as the sum of the individual conversions from esterification and transesterification, considering the contributions of each reaction to the total FAME production:

$$\%Total\ conversion = \%Esterification\ conversion + \%TG\ conversion \quad (6)$$

This approach allows for a more accurate determination of the total biodiesel output, accounting for the varying contributions from each reaction mechanism.

Table 5.
Total Conversion in Biodiesel Production Process.

Run	Total conversion (%)
1	86.7001
2	90.2976
3	85.9799
4	82.8082
5	85.7140
6	85.3281
7	88.0384
8	85.3435
9	87.1576
10	85.2995
11	88.1294
12	86.2231
13	84.6716
14	83.6397
15	89.4211
16	86.4984

According to Table 5, the highest total biodiesel conversion was achieved in the second experimental run, with a catalyst concentration of 2%, an operating temperature of 65°C, and a Fe/aluminosilicate catalyst ratio of 1:12, yielding a total conversion of 90.2976%. This result outperforms the findings of Muna et al. [36], who reported a yield of 89.23% using Fe/aluminosilicate catalysts in waste cooking oil transesterification. Furthermore, other studies involving transition metal impregnation in aluminosilicates have reported comparable yields: Ni/aluminosilicate catalysts produced a yield of 89.4% [37] while 5%Cu–1%Ru/BEA aluminosilicate catalysts achieved a yield of 85.7% [38]. These comparisons underscore the superior catalytic performance of iron in transition metal-impregnated aluminosilicate catalysts for biodiesel production. This study reveals that the method applied is highly effective in enhancing the production efficiency of biodiesel, with a conversion rate of up to 90.2976% from the initial FFA concentration of 20.68%. Optimizing the conversion to 90.2976% minimizes by-products, such as soap and glycerol residue, hence minimizing refining and processing waste costs. In industrial applications, this strategy has the potential to minimize production costs, especially with cheap material utilization [39].

The highest conversion was also achieved at a temperature of 65°C, which is considered optimal for the transesterification process. At lower temperatures, methanol remains in its subcritical state, leading to suboptimal conversion rates. Conversely, at temperatures exceeding 65°C, methanol tends to evaporate due to its boiling point of 64.96°C [40]. Methanol vaporization reduces its availability in the reaction medium, limiting its participation in the transesterification reaction. Additionally, the excess heat may lead to the formation of undesirable by-products, such as free fatty acids (FFAs), which can decrease the biodiesel yield by inhibiting transesterification and promoting side reactions such as saponification [41].

The optimization of reaction conditions for biodiesel production is vital for enhancing efficiency, reducing operational costs, and improving sustainability. Shorter reaction times not only reduce energy consumption but also minimize greenhouse gas emissions. Furthermore, process optimization techniques, such as Response Surface Methodology (RSM), offer greater control over the process, ensuring consistent product quality that meets industry standards. These advancements in process optimization contribute to making biodiesel production more economically viable and environmentally sustainable.

Optimizing catalyst concentration (2–4%) and reaction temperature (55–65°C) is critical for maximizing biodiesel production efficiency, scalability, and cost-effectiveness. A catalyst concentration of 2% generally yields the highest conversion while preventing issues such as saponification and excessive viscosity, which can lead to higher energy requirements for mixing [24, 25]. Higher temperatures accelerate reaction kinetics; however, temperatures exceeding 65°C may result in the evaporation of methanol, reducing efficiency [26]. By maintaining these optimal conditions, biodiesel production can achieve consistent product quality, lower operational costs, and support industrial scalability, ultimately improving the economic viability and sustainability of biodiesel manufacturing.

3.4. Optimization of Biodiesel Production Variables

Regression analysis, incorporating all independent variables and their interactions, was employed to determine the significance of various factors on the biodiesel yield. The response surface is mathematically represented by the following equation:

$$Y = 85{,}54 + 0{,}3119X_1 + 1{,}45X_2 + 0{,}8532X_3 - 0{,}3321X_1X_2 - 1{,}09X_1X_3 + 0{,}0736X_2X_3 + 0{,}5485X_1^2 + 0{,}5026X_2^2 - 0{,}1965X_3^3 \quad (7)$$

The equation expresses the combined effects of individual variables, their interactions, and their quadratic effects on the biodiesel yield.

As indicated in Table 2, the interactions between variables play a significant role in determining the biodiesel yield. The positive coefficients in the equation suggest that increasing the value of the corresponding independent variables leads to an increase in the response variable (total biodiesel conversion). Conversely, a negative coefficient indicates that increasing the independent variable will result in a decrease in the total biodiesel conversion. In particular, the coefficient of X_2 (operating temperature) is the largest at 1.45, suggesting that operating temperature has the most substantial impact on biodiesel conversion. Additionally, the coefficient for X_3 (Fe: aluminosilicate molar ratio) is also significant, but smaller than that of X_2, indicating that both higher operating temperature and higher Fe: aluminosilicate molar ratio positively influence the biodiesel yield.

Table 3 presents the statistical analysis of the regression model, with F-calculated values compared to their respective p-values. All single variables, squared variables, and interaction terms exhibit F-calculated values greater than their corresponding p-values, except for the interaction term X_2X_3 (operating temperature multiplied by Fe: aluminosilicate molar ratio). This suggests that, except for the interaction term X_2X_3, all other terms have a statistically significant impact on the total biodiesel conversion. Specifically, the linear terms for operating temperature (X_2) and Fe: aluminosilicate molar ratio (X_3) demonstrate significant effects due to their high F-values. The F-value for operating temperature (F=28.56) is notably higher than that for Fe: aluminosilicate molar ratio (F=9.94), which indicates that operating temperature has a more pronounced linear effect on biodiesel conversion.

Furthermore, the squared terms X_2^2 (operating temperature squared) and X_3^2 (Fe: aluminosilicate molar ratio squared) also exhibit significant effects on the response variable. The F-value for operating temperature squared (F=2.34) is higher than that for Fe: aluminosilicate molar ratio squared (F=0.3578), which again emphasizes the dominant influence of operating temperature on biodiesel conversion, even after considering the quadratic effects of both variables.

In summary, the regression analysis reveals that operating temperature (X^2) has the most significant effect on biodiesel conversion, followed by the Fe: aluminosilicate molar ratio (X^3). The interaction between these two variables, although not statistically significant, still has an observable influence, while the squared terms indicate the presence of nonlinear effects, further highlighting the importance of optimizing these factors for maximum biodiesel yield.

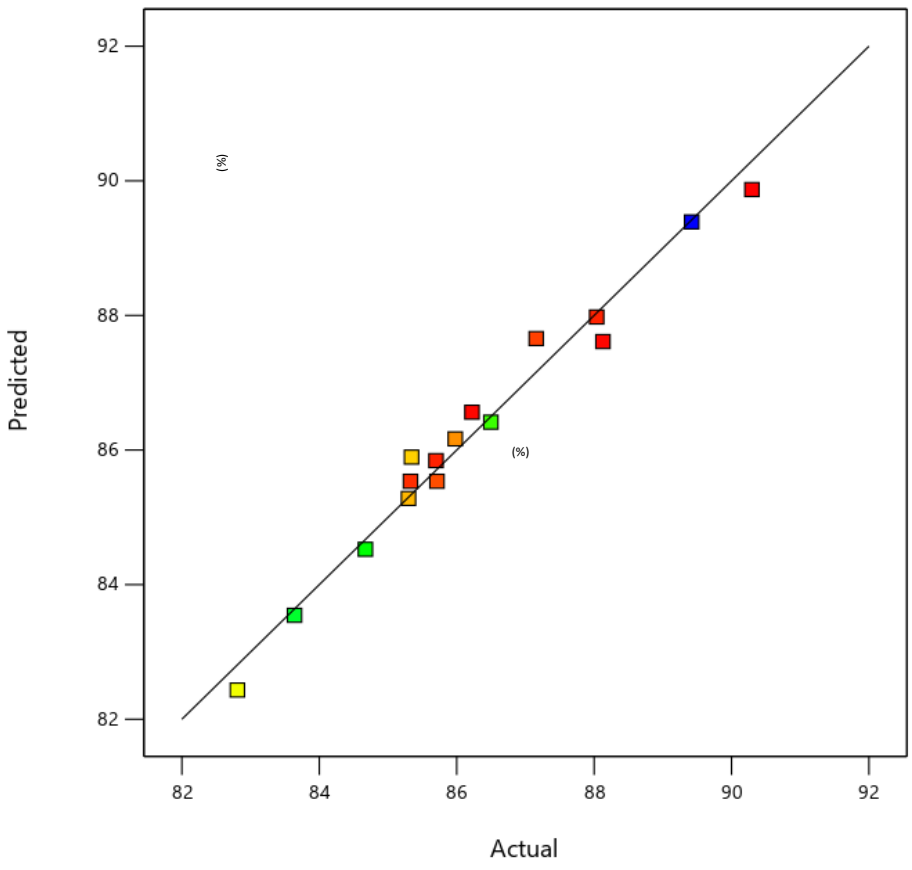


Figure 6.
Predicted vs actual total biodiesel conversion.

The quality of the mathematical model's fit is critically assessed through Analysis of Variance (ANOVA). A model is deemed satisfactory when the ANOVA results demonstrate a high level of statistical significance, indicating that the model can reliably predict the response variable. To determine the contribution of individual factors to the biodiesel yield, the p-value from the ANOVA analysis is used. Factors with low p-values (typically less than 0.05) are considered statistically significant, suggesting that they have a meaningful effect on the outcome.

In addition to ANOVA, further model validation is conducted by calculating the coefficient of determination (R^2), which measures the proportion of the total variation in the response variable (total biodiesel conversion) that can be explained by the independent variables included in the model [42]. A higher R^2 value indicates a better fit of the model, with values approaching 1.0 indicating that the model can explain nearly all of the observed variability.

In this experiment, the coefficient of determination (R^2) was found to be 0.9755. This implies that 97.55% of the variation in the total fatty acid methyl ester (FAME) conversion is accounted for by the independent variables in the model. Such a high R^2 value suggests that the model effectively captures the relationships between the independent variables and the response variable, providing a strong predictive capability. Conversely, the remaining 2.45% of the total variation in biodiesel conversion remains unexplained by the model, which could be attributed to factors not included in the analysis or inherent variability in the system.

Figure 6 illustrates the comparison between predicted and actual total biodiesel conversion, providing a visual validation of the model's predictive accuracy. The closeness of the predicted values to the actual data further supports the reliability of the model. Given the high R^2 value, the model is considered to be an effective tool for predicting the biodiesel conversion under the experimental conditions tested.

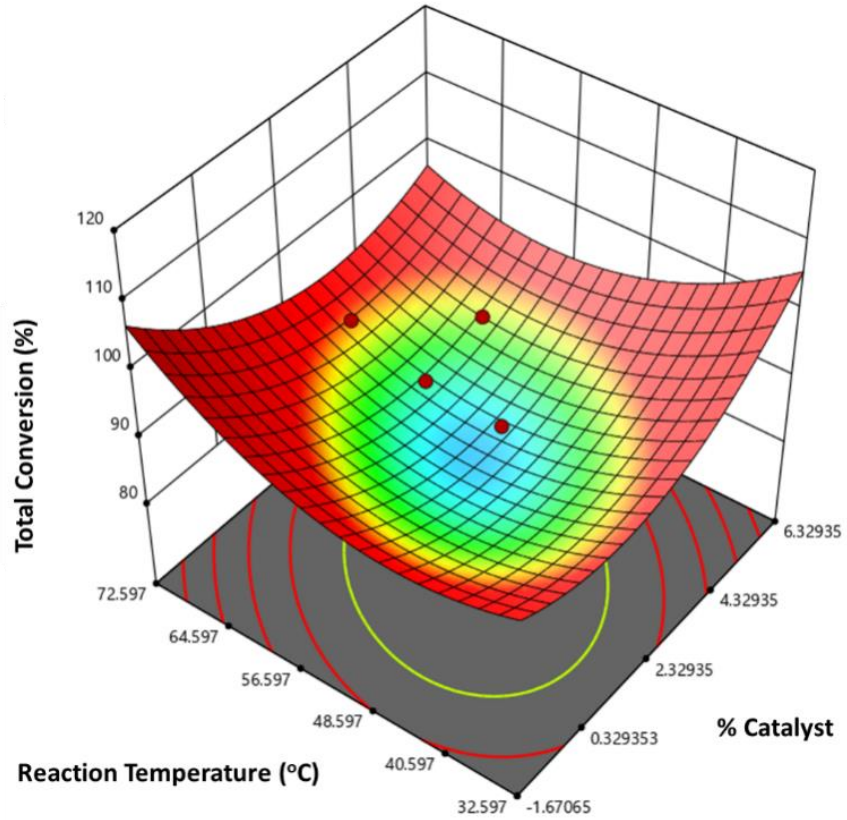


Figure 7.
3D Surface Model - Effect of %Catalyst and Reaction Temperature on Total Conversion.

Figure 7 presents a 3D response surface depicting the effect of varying catalyst concentrations and operating temperatures on the total biodiesel conversion. The data reveal that, at different operating temperatures, increasing the catalyst percentage enhances the total biodiesel conversion. However, when the catalyst concentration is held constant, an increase in operating temperature can lead to a decrease in biodiesel conversion.

According to Buchori et al. [43], increasing the catalyst concentration results in a higher number of active sites available for the reaction. A higher catalyst concentration improves the adsorption of methanol molecules, which facilitates the breaking of the hydroxyl (OH) bond, leading to the formation of methoxide ions. These methoxide ions then react with triglyceride molecules, producing biodiesel. This mechanism supports the positive correlation between catalyst concentration and biodiesel conversion observed at lower operating temperatures.

On the other hand, studies by Alismaeel et al. [44] suggest that increasing the operating temperature enhances catalyst molecular activity. At higher temperatures, catalyst molecules acquire sufficient energy to overcome the reaction's energy

barrier, thereby facilitating more efficient interactions with the reactants. As a result, this energy boost allows for greater conversion efficiency and an increase in biodiesel yield.

However, an excessively high catalyst concentration can negatively impact biodiesel conversion, as observed in the study by Yusuf et al. [45]. A high catalyst concentration can result in the formation of a thick slurry, which hinders effective mixing of the oil, methanol, and catalyst. This reduced mixing efficiency leads to suboptimal contact between the reactants, resulting in a decrease in biodiesel conversion. Consequently, while higher catalyst concentrations can improve biodiesel production to a certain extent, they can also lead to diminishing returns if the slurry becomes too thick to allow for efficient reaction kinetics.

In the present study, the optimal conditions for maximum biodiesel conversion were achieved at an operating temperature of 65°C and a catalyst concentration of 2%, yielding a total biodiesel conversion of 90.2976%. This highlights the importance of balancing both catalyst concentration and operating temperature to optimize biodiesel yield while avoiding complications associated with excessive catalyst concentration or suboptimal temperature conditions.

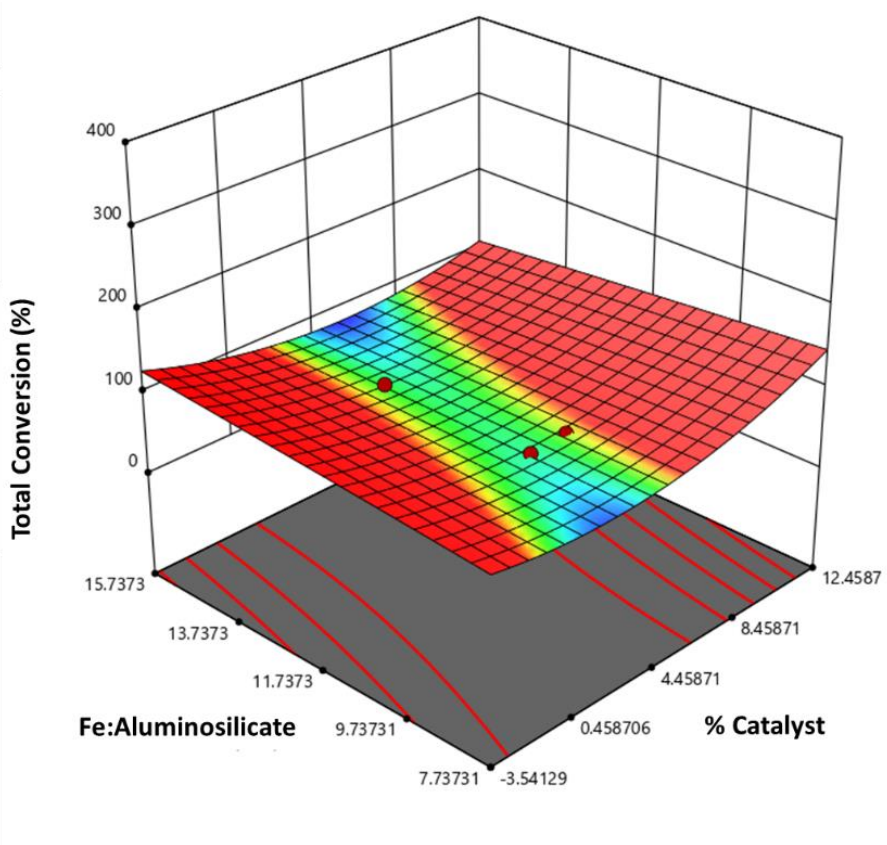


Figure 8.
3D Surface Model - Effect of % Catalyst and Fe:aluminosilicate Ratio on Total Conversion.

Figure 8 presents a 3D response surface illustrating the effect of varying catalyst percentages and Fe:aluminosilicate ratios on the total biodiesel conversion. The data indicate that, across various operating temperatures, an increase in the Fe:aluminosilicate ratio leads to a significant enhancement in total biodiesel conversion.

The catalytic activity and performance of Fe-based aluminosilicate catalysts in biodiesel production are significantly influenced by the distribution and impregnation of Fe within the aluminosilicate support. A uniform distribution of Fe ensures optimal exposure of active sites, enhancing the catalyst's activity, selectivity, and stability. Higher Fe content has been shown to improve catalytic performance, leading to increased biodiesel conversion, as Fe facilitates hydrogenation and transesterification reactions [19]. The optimal performance observed at a Fe/aluminosilicate ratio of 1:12 is due to the more homogeneous distribution of Fe, which maximizes interaction between methanol and triglycerides, thereby improving the yield of fatty acid methyl esters (FAME) and enhancing the overall efficiency of biodiesel production [46].

Fe is especially advantageous in aluminosilicate-based catalysts due to its role in hydrogenation reactions. Hydrogenation involves the reaction of esters (such as biodiesel) with hydrogen, which reduces the number of unsaturated bonds in the biodiesel molecule, thereby enhancing its stability [47]. This process is particularly valuable in improving biodiesel's oxidative stability and longevity. Furthermore, Fe plays a role in fatty acid chain cracking, a process wherein long-chain fatty acids are broken down into shorter chains. This cracking reaction, facilitated by the presence of Fe in the catalyst, results in biodiesel with improved fuel properties, such as lower viscosity and better combustion characteristics [48].

Iron (Fe), particularly in its oxide form (Fe_2O_3), exhibits hydrophobic properties that enhance its role as a heterogeneous catalyst in biodiesel production, particularly during esterification and transesterification reactions. The hydrophobic nature of Fe aids in the separation of fatty acid methyl esters (FAME) from the reaction mixture, improving FAME yield and overall biodiesel conversion efficiency. Fe accelerates the transesterification process by facilitating the nucleophilic attack of

methanol on triglycerides, resulting in higher conversion rates. Furthermore, the inherent basicity of Fe-based catalysts mitigates side reactions, such as saponification, by neutralizing free fatty acids (FFAs) and preventing their participation in soap formation, thus enhancing the overall efficiency of biodiesel production [49].

The optimal conditions observed in this experiment occurred at a Fe:aluminosilicate molar ratio of 1:12 and a catalyst concentration of 2%, which resulted in a total biodiesel conversion of 90.2976%. These results underscore the importance of optimizing both the Fe:aluminosilicate ratio and catalyst concentration to achieve maximal biodiesel yield. The presence of Fe in the aluminosilicate catalyst enhances reaction rates, promotes desirable side reactions, and increases the overall efficiency of biodiesel production.

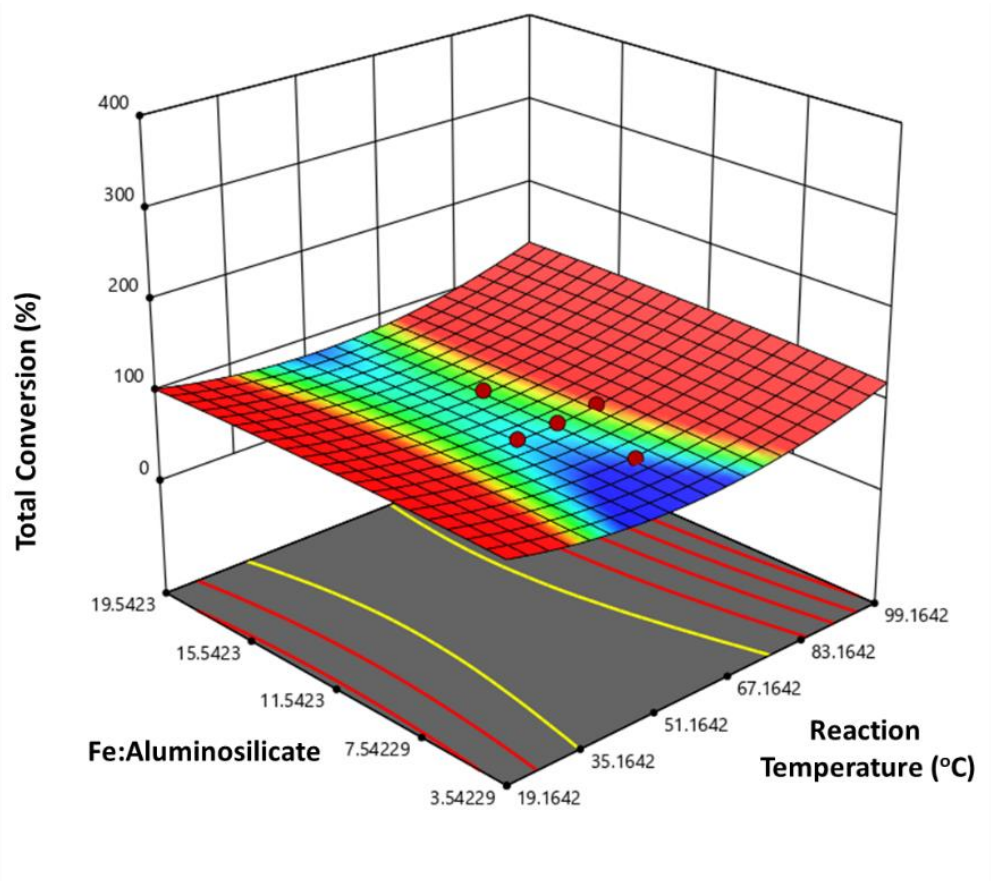


Figure 9.
3D Surface Model - Effect of Reaction Temperature and Fe : aluminosilicate Ratio on Total Conversion.

Figure 9 presents a 3D response surface illustrating the effect of varying operating temperatures and Fe: aluminosilicate ratios on total biodiesel conversion. The data reveal that, across different Fe:aluminosilicate ratios, increasing the operating temperature leads to a marked increase in total biodiesel conversion.

Operating temperature is a critical factor in biodiesel production as it significantly influences the reaction kinetics. At higher temperatures, the molecules gain more kinetic energy, increasing their movement and the frequency of molecular collisions. This enhanced molecular activity accelerates the rate of transesterification, thereby reducing the overall reaction time required to produce biodiesel [50]. Specifically, elevated temperatures facilitate the conversion of triglycerides to methyl esters by decreasing the viscosity of the oil. Lower viscosity allows for better molecular mobility, increasing the number of effective collisions between reactant molecules, which in turn speeds up the reaction rate [51].

Moreover, higher temperatures improve the solubility of methanol in the reaction mixture, further promoting the transesterification process. By enhancing the molecular interactions between methanol and triglycerides, elevated temperatures lead to a more efficient and faster production of biodiesel.

The optimal results in this study were achieved at an operating temperature of 65°C and a Fe:aluminosilicate molar ratio of 1:12, yielding a total biodiesel conversion of 90.2976%. These findings emphasize the importance of carefully optimizing both the operating temperature and catalyst ratio to maximize biodiesel production efficiency while maintaining reaction efficacy.

3.5. Characteristics of Biodiesel

The performance of catalysts in esterification-transesterification reactions can be assessed through various biodiesel characteristics, including density, viscosity, and free fatty acid (FFA) content. These parameters serve as key indicators of biodiesel quality and are evaluated according to established standards, such as those specified in SNI 718:2015. The standards

include values for density and viscosity, which are essential for determining the fuel properties of biodiesel. A summary of the biodiesel characteristics produced in the experiment is provided in Table 5.

Table 6.
Characteristics of experimental biodiesel.

Run / SNI	Density (gr/ml)	Viscosity (cSt)	%FFA
	0.85-0.9	**2.3-6**	
1	0.86298	0.90135	4.41798
2	0.85467	0.73037	3.51520
3	0.88169	1.52785	5.15263
4	0.88828	1.93990	5.20759
5	0.86995	1.21840	4.85275
6	0.89282	2.73398	5.90646
7	0.86536	1.04763	4.59715
8	0.88827	1.85554	5.20765
9	0.86642	1.09005	4.68144
10	0.88516	1.70196	5.13243
11	0.86046	0.75574	3.58209
12	0.86222	0.83916	4.42188
13	0.89046	2.70562	5.37529
14	0.89296	3.24314	6.36358
15	0.89694	3.25759	6.51450
16	0.89025	2.38799	5.37656

From the data presented in Table 6, it is evident that both PAO-bulk oil and Fe/aluminosilicate catalysts are effective in the production of biodiesel. Notably, the FFA content in the PAO-bulk oil feedstock was significantly reduced after conversion to biodiesel, from an initial value of 20.68% to a final range of 3-6%. This substantial reduction in FFA content underscores the high catalytic efficiency of the Fe/aluminosilicate catalyst in converting free fatty acids into fatty acid methyl esters (FAME), which are the main constituents of biodiesel.

The reduction in FFA is particularly significant as it demonstrates the catalyst's ability to efficiently catalyze both esterification and transesterification reactions, ensuring that a higher proportion of triglycerides and free fatty acids are converted to biodiesel. This is a key indicator of the catalyst's effectiveness in the biodiesel production process, as it minimizes the formation of undesirable byproducts such as soap and ensures a high biodiesel yield. The results suggest that Fe/aluminosilicate catalysts are highly effective in producing biodiesel with desirable physicochemical properties that comply with biodiesel standards.

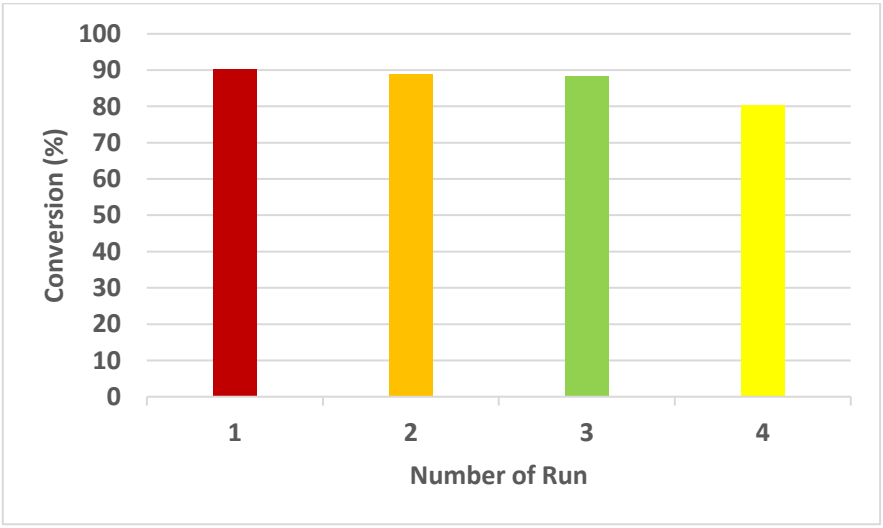


Figure 10.
Reusability of Fe/aluminosilicate Catalyst.

3.6. Reusability Catalyst

Catalyst reusability performance was evaluated by conducting biodiesel production under the second experiment condition (2% catalyst, temperature 65 °C). Before being utilized in the subsequent cycle, the catalyst was separated from the product, rinsed with n-hexane, and dried in an oven for six hours. Figure 10 illustrates the reusability of the Fe/aluminosilicate catalyst. As can be seen from the graphic above, the catalyst was active for three cycles without a

significant drop in %conversion. However, a significant drop was found in the fourth cycle. This phenomenon is attributed to catalyst structure degradation. The leaching of Fe particles during the trans-esterification process leads to the degradation of the catalyst structure. Repeated use of the catalyst modifies the catalyst crystal structure and porosity, which reduces the catalytic activity [52]. Furthermore, a reduction in % conversion may take place as a result of the accumulation of fatty acids, glycerol, or glycerides (including triglycerides, diglycerides, and monoglycerides) on the active sites [53].

Based on the data provided, the test catalyst showed an initial biodiesel conversion of 90.298%, which decreased slightly after several reuse cycles, reaching 80.365% in the fourth cycle. In comparison to commercial heterogeneous catalysts like CaO, MgO, or ZnO, which are capable of being reused for 5–10 cycles with a conversion decrease of approximately 3–10% per cycle, the reusability test demonstrated competitive performance, even though it faced a significant reduction during the fourth cycle [54-56]. This investigation demonstrated that the catalyst demonstrated that Fe/aluminosilicate exhibited a slow reduction in %conversion after multiple cycles, maintaining biodiesel conversion above 80% until the fourth cycle. This suggests that Fe/aluminosilicate retains good activity, allowing for reuse without frequent synthesis, thus contributing to cost and energy efficiency in biodiesel production. Further study in catalyst modification, regeneration techniques, and optimization of reaction operations is essential for the Fe/aluminosilicate catalyst to effectively compete with commercial heterogeneous catalysts in industrial applications.

4. Conclusion

This study successfully synthesized a heterogeneous Fe/aluminosilicate catalyst via the impregnation method, utilizing iron sand and geothermal waste-derived aluminosilicate. Characterization through SEM-EDX confirmed uniform Fe distribution, while XRD identified SiO_2 (tridymite phase) and Fe_2O_3 (hematite phase). The optimal conditions for biodiesel production were determined to be 2% Fe/aluminosilicate catalyst concentration, 65°C reaction temperature, and a 1:12 Fe:aluminosilicate ratio, achieving a high biodiesel conversion of 90.2976%. The produced biodiesel met SNI 7182:2015 standards in terms of density, viscosity, and free fatty acid (FFA) content. Future studies should explore other quality parameters, including cetane number and oxidative stability, to ensure fuel reliability. Furthermore, conducting a life-cycle assessment (LCA) of Fe/aluminosilicate-based biodiesel production would be beneficial in quantifying its environmental impact compared to traditional biodiesel synthesis methods.

References

[1] H. Yang *et al.*, "Satellite-observed strong subtropical ocean warming as an early signature of global warming," *Communications Earth & Environment*, vol. 4, no. 1, p. 178, 2023. https://doi.org/10.1038/s43247-023-00839-w

[2] J. Lelieveld, K. Klingmüller, A. Pozzer, R. Burnett, A. Haines, and V. Ramanathan, "Effects of fossil fuel and total anthropogenic emission removal on public health and climate," *Proceedings of the National Academy of Sciences*, vol. 116, no. 15, pp. 7192-7197, 2019. https://doi.org/10.1073/pnas.1819989116

[3] S. Vellaiyan, M. Kandasamy, B. Nagappan, S. Gupta, K. Ramalingam, and Y. Devarajan, "Optimization study for efficient and cleaner production of waste-derived biodiesel through fuel modification and its validation," *Process Integration and Optimization for Sustainability*, vol. 8, no. 3, pp. 939-952, 2024. https://doi.org/10.1007/s41660-024-00404-8

[4] R. Kolobeng, C. Ketlogetswe, M. Jonas, and D. Mautle, "Effects of moisture content on biodiesel (B100) properties during storage: A comparative analysis between biodiesel produced from used cooking oil and beef tallow," *Sustainable Energy Technologies and Assessments*, vol. 54, p. 102844, 2022. https://doi.org/10.1016/j.seta.2022.102844

[5] P. Dalvand and L. Mahdavian, "Biodiesel production in the presence of eggshell nano-catalyst," *Chemistry and Technology of Fuels and Oils*, vol. 58, no. 1, pp. 55-62, 2022. https://doi.org/10.1007/s10553-022-01351-1

[6] F. A. Ishak, M. H. Jamil, A. S. Abd Razak, N. H. A. Zamani, and M. R. Ab Hamid, "Development of animal feed from waste to wealth using napier grass and palm acid oil (PAO) from palm oil mill effluent (POME)," *Materials Today: Proceedings*, vol. 19, pp. 1618-1627, 2019. https://doi.org/10.1016/j.matpr.2019.11.190

[7] H. Noge, Y. Ueno, H. A. Kadir, and W. J. Yahya, "Utilization of palm acid oil for a diffusion combustion burner as fuel and nitrogen oxides reduction by the thermally decomposed hydrocarbons," *Energy*, vol. 224, p. 120173, 2021. https://doi.org/10.1016/j.energy.2021.120173.

[8] K. A. Zahan and M. Kano, "Biodiesel production from palm oil, its by-products, and mill effluent: A review," *Energies*, vol. 11, no. 8, p. 2132, 2018. https://doi.org/10.3390/en11082132.

[9] J. Rizkiana, B. Bryan, E. Gozali, A. T. A. Bustomi, and T. Prakoso, "Hematite-Gamma Alumina-based solid catalyst development for biodiesel production from Palm Oil," *Journal of Engineering and Technological Sciences*, vol. 56, no. 1, pp. 50-60, 2024. https://doi.org/10.5614/j.eng.technol.sci.2024.56.1.4

[10] M. Bayramoilu, I. Korkut, and B. T. Ergan, "Reusability and regeneration of solid catalysts used in ultrasound assisted biodieselproduction," *Turkish Journal of Chemistry*, vol. 45, no. 2, pp. 342-347, 2021. https://doi.org/10.3906/KIM-2008-33.

[11] A. Martínez, G. E. Mijangos, I. C. Romero-Ibarra, R. Hernández-Altamirano, V. Y. Mena-Cervantes, and S. Gutiérrez, "A novel green one-pot synthesis of biodiesel from Ricinus communis seeds by basic heterogeneous catalysis," *Journal of Cleaner Production*, vol. 196, pp. 340-349, 2018. https://doi.org/10.1016/j.jclepro.2018.05.241

[12] R. Nayab *et al.*, "Sustainable biodiesel production via catalytic and non-catalytic transesterification of feedstock materials–A review," *Fuel*, vol. 328, p. 125254, 2022. https://doi.org/10.1016/j.fuel.2022.125254

[13] F. Jamil *et al.*, "Biodiesel production by valorizing waste Phoenix dactylifera L. Kernel oil in the presence of synthesized heterogeneous metallic oxide catalyst (Mn@ MgO-ZrO2)," *Energy Conversion and Management*, vol. 155, pp. 128-137, 2018. https://doi.org/10.1016/j.enconman.2017.10.064.

[14] A. I. Osman *et al.*, *Optimizing biomass pathways to bioenergy and biochar application in electricity generation, biodiesel production, and biohydrogen production*. Switzerland: Springer International Publishing, 2023.

[15] J. Zhang *et al.*, "Synthesis, characterization and application of Fe-zeolite: A review," *Applied Catalysis A: General*, vol. 630, p. 118467, 2022. https://doi.org/10.1016/j.apcata.2021.118467

[16] N. S. Lani, N. Ngadi, I. M. Inuwa, L. A. Opotu, Z. Y. Zakaria, and W. Widayat, "Influence of desilication route of ZSM-5 zeolite in mesoporous zeolite supported calcium oxide catalyst for biodiesel production," *Microporous and Mesoporous Materials*, vol. 343, p. 112153, 2022. https://doi.org/10.1016/j.micromeso.2022.112153

[17] V. Gupta and K. P. Singh, "The impact of heterogeneous catalyst on biodiesel production; A review," *Materials Today: Proceedings*, vol. 78, pp. 364-371, 2023. https://doi.org/10.1016/j.matpr.2022.10.175

[18] W. Widayat *et al.*, "Production of biodiesel from waste cooking oil using heterogeneous catalysts KI/γ-Al2O3," *Journal of Environmental Engineering and Science*, vol. 15, no. 3, pp. 107-112, 2020. https://doi.org/10.1680/jenes.19.00012

[19] A. Fakruldin, A. Ramli, and M. I. A. Mutalib, "Effect of preparation method on physicochemical properties of Fe/zeolite catalyst," *Journal of Physics: Conference Series, IOP Publishing*, vol. 1123, no. 1, p. 012061, 2018. https://doi.org/10.1088/1742-6596/1123/1/012061

[20] W. Widayat, J. Philia, T. Farsha, and F. Rifaldi, "Synthesis of zeolite catalyst from geothermal solid waste for crude glycerol dehydration to acrolein," *Key Engineering Materials*, vol. 849, pp. 130-136, 2020.

[21] R. Wahyudityo, A. W. Harto, and K. Suryopratomo, "Silica scaling analysis on brine injection pipe in dieng geothermal field with case study at PT. Geo Dipa Energi," *Teknofisika*, vol. 2, no. 1, pp. 7-14, 2013.

[22] F. A. Setiawan, E. Rahayuningsih, H. T. B. M. Petrus, M. I. Nurpratama, and I. Perdana, "Kinetics of silica precipitation in geothermal brine with seeds addition: Minimizing silica scaling in a cold re-injection system," *Geothermal Energy*, vol. 7, no. 1, p. 22, 2019. https://doi.org/10.1186/s40517-019-0138-3

[23] J. Prameswari, W. Widayat, L. Buchori, and H. Hadiyanto, "Novel iron sand-derived α-Fe2O3/CaO2 bifunctional catalyst for waste cooking oil-based biodiesel production," *Environmental Science and Pollution Research*, vol. 30, no. 44, pp. 98832-98847, 2023. https://doi.org/10.1007/s11356-022-21942-z

[24] A. B. Hossain and M. Mazen, "Effects of catalyst types and concentrations on biodiesel production from waste soybean oil biomass as renewable energy and environmental recycling process," *Australian Journal of Crop Science*, vol. 4, no. 7, pp. 550-555, 2010.

[25] W. Wendi, "Effect of reaction temperature and catalyst concentration," presented at the 5th Sriwijaya International Seminar on Energy and Environmental Science and Technology. Sriwijaya University, 2014.

[26] S. B. Masango, P. T. Ngema, O. A. Olagunju, and S. Ramsuroop, "The effect of reaction temperature, catalyst concentration and alcohol ratio in the production of biodiesel from raw and purified castor oil," *Advances in Chemical Engineering and Science*, vol. 14, no. 3, pp. 137-154, 2024. https://doi.org/10.4236/aces.2024.143009

[27] Ganet Academy, *Gannet academy central composite design*. Nigeria: Ganet Academy Publications, 2020.

[28] O. C. Chiedu *et al.*, "Central composite design optimization of the extraction and transesterification of tiger nut seed oil to biodiesel," *Process Integration and Optimization for Sustainability*, vol. 8, no. 2, pp. 503-521, 2024. https://doi.org/10.1007/s41660-023-00379-y

[29] V. Seithtanabutara, C. Sungnat, and T. Wongwuttanasatian, "Comparison of free fatty acid conversion yields for esterification assisted by single-and dual-frequency sonication," *Biomass Conversion and Biorefinery*, vol. 11, pp. 2585-2597, 2021. https://doi.org/10.1007/s13399-020-00659-4

[30] R. Putra, W. W. Lestari, F. R. Wibowo, and B. H. Susanto, "Fe/Indonesian natural zeolite as hydrodeoxygenation catalyst in green diesel production from palm oil," *Bulletin of Chemical Reaction Engineering & Catalysis*, vol. 13, no. 2, pp. 245-255, 2018. https://doi.org/10.9767/bcrec.13.2.1382.245-255

[31] Y. Li, J. Dang, Y. Ma, and H. Ma, "Hematite: A good catalyst for the thermal decomposition of energetic materials and the application in nano-thermite," *Molecules*, vol. 28, no. 5, p. 2035, 2023. https://doi.org/10.3390/molecules28052035

[32] Y. Yu, W. J. Movick, K. Obata, S. Yoshida, and K. Takanabe, "Mn-Na2WO4/SiO2-tridymite with improved stability and selectivity for high-pressure oxidative coupling of methane," *Chemical Engineering Journal*, vol. 500, p. 156938, 2024. https://doi.org/10.1016/j.cej.2024.156938

[33] J. Philia, W. Widayat, S. Sulardjaka, G. A. Nugroho, and A. N. Darydzaki, "Aluminum-based activation of natural zeolite for glycerol steam reforming," *Results in Engineering*, vol. 19, p. 101247, 2023. https://doi.org/10.1016/j.rineng.2023.101247

[34] P. X. W. Zou, L. Zhang, and Y. Xu, "Risk management in construction projects: A systematic review," *International Journal of Project Management*, vol. 38, no. 3, pp. 185-195, 2020. https://doi.org/10.1016/j.ijproman.2019.11.008

[35] V. Sidi Neto, S. Derenzo, M. P. d. A. Marin, L. F. Novazzi, and J. G. R. Poco, "Biodiesel production from vegetal oil and ethanol via transesterification in supercritical conditions," *Brazilian Journal of Chemical Engineering*, vol. 41, no. 3, p. 0123456789, 2024. https://doi.org/10.1007/s43153-023-00379-y

[36] N. L. Muna, A. A. Mu'alimah, D. B. Pridiana, A. K. Widodo, S. R. Adiyar, and E. H. Elinda, "The production of biodiesel from waste cooking oil (simultaneous esterification and transesterification using Fe/zeolite catalysts from waste geothermal)," *Materials Science Forum*, vol. 990, pp. 161–167, 2020.

[37] H. Satriadi, I. Y. Pratiwi, M. Khuriyah, and J. Prameswari, "Geothermal solid waste derived Ni/Zeolite catalyst for waste cooking oil processing," *Chemosphere*, vol. 286, p. 131618, 2022. https://doi.org/10.1016/j.chemosphere.2021.131618

[38] Ł. Szkudlarek, K. Chałupka-Śpiewak, W. Maniukiewicz, J. Albińska, M. I. Szynkowska-Jóźwik, and P. Mierczyński, "Biodiesel production via transesterification reaction over mono-and bimetallic copper-noble metal (Pt, Ru) catalysts supported on BEA Zeolite," *Catalysts*, vol. 14, no. 4, p. 260, 2024. https://doi.org/10.3390/catal14040260

[39] S. Banga and V. V. Pathak, "Biodiesel production from waste cooking oil: A comprehensive review on the application of heterogenous catalysts," *Energy Nexus*, vol. 10, p. 100209, 2023. https://doi.org/10.1016/j.nexus.2023.100209

[40] M. G. Weldeslase, N. E. Benti, M. A. Desta, and Y. S. Mekonnen, "Maximizing biodiesel production from waste cooking oil with lime-based zinc-doped CaO using response surface methodology," *Scientific Reports*, vol. 13, no. 1, p. 4430, 2023. https://doi.org/10.1038/s41598-023-30961-w

[41] M. Andrifar, F. Goembira, M. Ulfah, R. Putri, R. Yuliarningsih, and R. Aziz, "Optimization of sustainable biodiesel production from waste cooking oil using heterogeneous alkali catalyst," *Jurnal Rekayasa Proses*, vol. 16, no. 2, pp. 141-146, 2022. https://doi.org/10.22146/jrekpros.74373

[42] C. E. Akhabue, U. J. Ukponahiusi, E. O. Osa-Benedict, S. K. Otoikhian, O. C. Inetianbor, and E. A. Oyedoh, "Simultaneous esterification and transesterification of neem seed oil using ferric sulphate doped with poultry droppings as a bifunctional catalyst," *Frontiers in Energy Research*, vol. 10, pp. 1-11, 2022. https://doi.org/10.3389/fenrg.2022.927467

[43] L. Buchori, W. Widayat, O. Muraza, M. I. Amali, R. W. Maulida, and J. Prameswari, "Effect of temperature and concentration of zeolite catalysts from geothermal solid waste in biodiesel production from used cooking oil by esterification–transesterification process," *Processes*, vol. 8, no. 12, pp. 1–16, 2020. https://doi.org/10.3390/pr8121629

[44] Z. T. Alismaeel, T. M. Al-Jadir, T. M. Albayati, A. S. Abbas, and A. M. Doyle, "Modification of FAU zeolite as an active heterogeneous catalyst for biodiesel production and theoretical considerations for kinetic modeling," *Advanced Powder Technology*, vol. 33, no. 7, p. 103646, 2022. https://doi.org/10.1016/j.apt.2022.103646

[45] B. O. Yusuf, S. A. Oladepo, and S. A. Ganiyu, "Zr-modified desilicated ZSM-5 catalysts as highly active and recyclable catalysts for production of biodiesel from soybean oil: Insight into improved catalyst properties, acidity and dispersion through desilication," *Fuel*, vol. 351, p. 128729, 2023. https://doi.org/10.1016/j.fuel.2023.128729

[46] X. Wang, C. Jiang, J. Wang, K. Gui, and H. R. Thomas, "Promoted dispersion and uniformity of active species on Fe–Ce–Al catalysts for efficient NO abatement," *RSC Advances*, vol. 9, no. 61, pp. 35751-35759, 2019. https://doi.org/10.1039/c9ra06875a

[47] A. Masudi, O. Muraza, N. W. C. Jusoh, and U. Ubaidillah, "Improvements in the stability of biodiesel fuels: recent progress and challenges," *Environmental Science and Pollution Research*, vol. 30, no. 6, pp. 14104-14125, 2023. https://doi.org/10.1007/s11356-022-25048-4

[48] A. Santoso, R. Joharmawan, and L. B. Hutami, "Catalytic cracking of waste frying oil using Ni-Fe/activated zeolite catalyst as a source of renewable energy," *IOP Conference Series: Materials Science and Engineering*, *IOP Publishing*, vol. 509, no. 1, p. 012009, 2019. https://doi.org/10.1088/1757-899X/509/1/012009

[49] I. Rizwanul Fattah *et al.*, "State of the art of catalysts for biodiesel production," *Frontiers in Energy Research*, vol. 8, pp. 1–17, 2020. https://doi.org/10.3389/fenrg.2020.00101

[50] I. K. Ajadi, T. Oyegoke, T. T. Geoffrey, O. Fasanya, and A. O. Ojetunde, "Biodiesel production from neem seed oil: Catalyst synthesis, effect of time, and temperature on biodiesel yield," *Proceedings of the Materials Science and Technology Society of Nigeria*, vol. 1, pp. 45–52, 2021.

[51] Triyono, W. Trisunaryanti, S. I. Aksanti, and J. Purbonegoro, "High performance of a base catalyst from Moringa leaves ash for biodiesel conversion of low-grade Bali Malapari oil," *Reaction Kinetics, Mechanisms and Catalysis*, vol. 137, no. 4, pp. 2037-2063, 2024. https://doi.org/10.1007/s11144-024-02637-7

[52] L. Buchori, W. Widayat, H. Hadiyanto, H. Satriadi, N. Chasanah, and M. R. Kurniawan, "Modification of magnetic nanoparticle lipase catalyst with impregnation of Activated Carbon Oxide (ACO) in biodiesel production from PFAD (Palm Fatty Acid Distillate)," *Bioresource Technology Reports*, vol. 19, p. 101137, 2022. https://doi.org/10.2139/ssrn.4049412

[53] N. Zhang, H. Xue, and R. Hu, "The activity and stability of CeO 2@ CaO catalysts for the production of biodiesel," *RSC Advances*, vol. 8, no. 57, pp. 32922-32929, 2018. https://doi.org/10.1039/c8ra06884d

[54] S. F. Basumatary *et al.*, "Advances in CaO-based catalysts for sustainable biodiesel synthesis," *Green Energy and Resources*, vol. 1, no. 3, p. 100032, 2023. https://doi.org/10.1016/j.gerr.2023.100032

[55] V. Gadore, S. R. Mishra, N. Yadav, G. Yadav, and M. Ahmaruzzaman, "Metal oxide-based heterogeneous catalysts for biodiesel production," *Next Sustainability*, vol. 2, p. 100012, 2023. https://doi.org/10.1016/j.nxsust.2023.100012

[56] R. Jayabal, "Advancements in catalysts, process intensification, and feedstock utilization for sustainable biodiesel production," *Results in Engineering*, vol. 24, p. 103668, 2024. https://doi.org/10.1016/j.rineng.2024.103668